

Load-Bearing Actuator with Permanent Magnet for Transport of Rails

Abstract. A new solution for transporting long ferromagnetic bodies is presented, based on a system of permanent magnets whose attractive force at the moment of releasing the load is reduced by pulse magnetic field produced by appropriately arranged coils. The continuous mathematical model of the device is solved numerically. Its operation characteristics illustrated by an example are evaluated and discussed.

Streszczenie. W artykule przedstawiono metodę transportu długich obiektów ferromagnetycznych. W rozwiązaniu wykorzystane zostało zjawisko osłabiania siły z jaką magnesy trwale przyciągają obciążenie, poprzez wytworzenie impulsowego pola magnetycznego, wytworzonego przez odpowiednio ustawione cewki. Zastosowano model matematyczny urządzenia o dziedzinie ciągłej, który poddano analizie numerycznej. Przedstawiono i omówiono wynikowe charakterystyki pracy. (Słownik nośny z magnesami trwałymi to transportu szyn).

Keywords: transport of ferromagnetic bodies, permanent magnet, magnetic field, numerical analysis

Słowa kluczowe: transport korpusów ferromagnetycznych, magnesy trwale, pole magnetyczne, analiza numeryczna.

Introduction

Transport of long massive steel bodies (for example rails, rods or pipes) is commonly realized by mobile cranes to which such bodies are fastened by steel ropes. The process of their binding and manipulation with them, however, are laborious and dangerous. That is why new possibilities in the domain are intensively looked for. The paper represents an introductory study of a fixing device for transport of steel rails (or other long bodies) equipped with a system of load-bearing transport actuators with permanent magnets producing the necessary attractive force. The device does not need any external source of electric energy. It just works with short current pulses (causing a short-time demagnetization of the permanent magnets) at the moment of releasing the body that may be, for example, delivered from a sufficiently powerful capacitor battery mounted on the device.

The arrangement of the actuator is depicted in Fig. 1. Its principal parts are the permanent magnet 1, ferromagnetic shell 2 and demagnetization coil 3 placed in an insulation shell 4. The position of the permanent magnet is fixed by two spacers 5.1 and 5.2. Position 6 shows the transported body, in this case a steel rail. The actuator itself (consisting of parts described by positions 1–5.2) can be either cylindrical or prismatic. More advantageous, however, is the prismatic version because it allows for a substantially wider variability of the system.

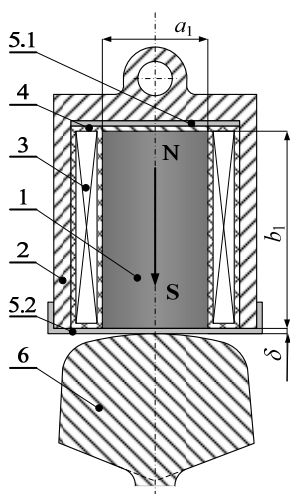


Fig. 1. Basic arrangement of the load-bearing actuator with permanent magnet

Operation of the actuator is characterized by two regimes. The first one is the regime “on” that represents fixing of the transported body. The total attractive force produced by the system of permanent magnets in the individual actuators must exceed (with a prescribed safety coefficient) the weight of the body. Fixing of the ferromagnetic body 6 to the shell 2 is realized by mere approaching of the fixing device to it. The coils 3 carry no currents. The second one is the regime “off” when the body is released. Now short current pulses of density J_{off} are delivered to the coils, whose magnetic fields act against the magnetic fields of the permanent magnets. The permanent magnets are demagnetized and their total attractive force decreases to a value smaller than the weight of the body. In this way, the body is released and falls slowly down.

The permanent magnets should be made of material with a low electric conductivity in order to avoid producing eddy currents at the moment of their “switching off” and their demagnetization must be limited by the straight part of their demagnetization characteristic in order to avoid deteriorating their physical parameters.

The aim of the paper is to model the operation characteristics of the device.

Mathematical model

A general equation describing the field in the considered load-bearing element with a permanent magnet reads (see [1], [2])

$$(1) \quad \text{curl} \left(\frac{1}{\mu} (\text{curl} \mathbf{A}) - \mathbf{H}_c \right) = \mathbf{J}_{off}$$

where \mathbf{A} is the magnetic vector potential, \mathbf{H}_c stands for the coercivity of the permanent magnet, μ denotes the permeability and \mathbf{J}_{off} is the appropriately oriented current density in the releasing coil (this density is only nonzero during the process of releasing the load). The conditions along a sufficiently distant boundary are of the Dirichlet type ($\mathbf{A} = \mathbf{0}$).

The corresponding vector \mathbf{F} of the attractive force acting on the rail by the load-fixing element is given by the integral [2]

$$(2) \quad \mathbf{F} = \frac{1}{2} \oint_C (\mathbf{H} (\mathbf{n} \cdot \mathbf{B}) + \mathbf{B} (\mathbf{n} \cdot \mathbf{H}) - \mathbf{n} (\mathbf{H} \cdot \mathbf{B})) dC$$

where \mathbf{H} and \mathbf{B} are the field vectors, \mathbf{n} is the unit vector of the outward normal and integration is carried out along the whole surface C of the rail.

Illustrative example

We investigated the behaviour and operation properties of a prismatic device (the cross section of the permanent magnet being $a_1 \times b_1$ (see Fig. 1) and its length in the direction z being l_1) in two variants shown in Fig. 2.

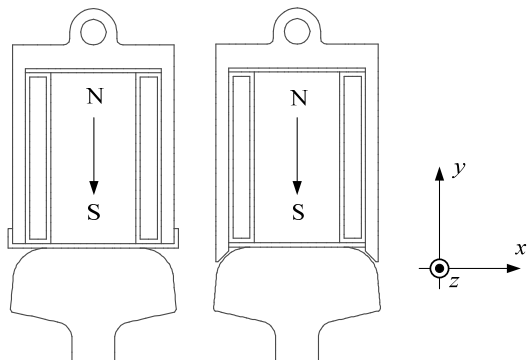


Fig. 2. Two considered versions of the device (left – basic arrangement, right – improved shape of the shell providing a thinner gap between the permanent magnet and rail)

The permanent magnet was chosen with respect to the above requirements (mainly low electric conductivity). After the evaluation of basic physical properties of several common materials we used commercially available magnet of type NEOREC 53B [3]. The most important part of its demagnetization characteristic (that is practically linear) is depicted in Fig. 3.

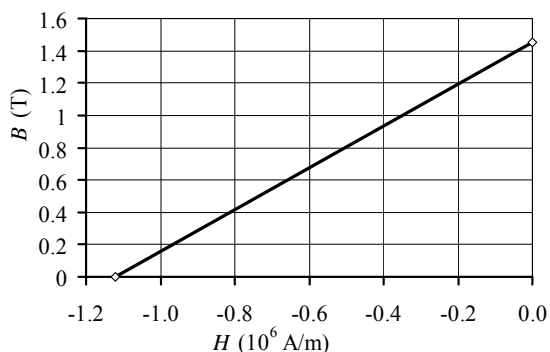


Fig. 3. Demagnetization curve of permanent magnet NEOREC 53B ($B_r = 1.452 \pm 0.02$ T, $H_c = -1120 \pm 48$ kA/m)

The magnetic shell **2** is made of standard carbon steel CSN 12 040 [4] whose nonlinear magnetization characteristic is shown in Fig. 4.

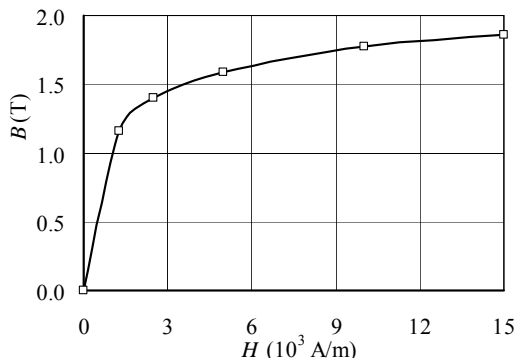


Fig. 4. Nonlinear magnetization characteristic $B(H)$ of carbon steel CSN 12 040

The gap of thickness δ (see Fig. 1) is variable, similarly as the dimensions a_1 , b_1 and l_1 of the prismatic magnet and number n of the devices.

The numerical solution of the model (1) was realized by the finite element method-based code QuickField [5] supplemented with a number of our own procedures and scripts. All physical properties of particular materials (the real characteristics of steel CSN 12 040 and permanent magnet NEOREC 53B) were taken into account. A special attention was paid to the convergence of the results on the position of the artificial boundary and density of the discretization mesh (we checked the average magnetic field in the permanent magnet **1** and force acting on the transported body. For example, Tab. 1 shows such values for the improved arrangement depicted in the right part of Fig. 2 under the specified conditions, provided that the length of the permanent magnet $l_1 = 1$ m.

Table 1. Convergence of the solution for the improved arrangement: $b_1 / a_1 = 80 / 40$ mm, $\delta = 2$ mm, $J_{\text{off}} = 0$, $l_1 = 1$ m.

mesh number of nodes	results		
	F [kN]	B_{avrg} [T]	H_{avrg} [10^5 A/m]
12968	30.258	1.2204	9.429
51576	30.637	1.2208	9.432
204977	30.707	1.2209	9.433

Here, F denotes the force exerted by one permanent magnet on the rail, while B_{avrg} and H_{avrg} stand for the average magnetic flux density and magnetic field strength in the permanent magnet, respectively.

Now we will present the most important results (related to the length of permanent magnet $l_1 = 1$ m).

Figs. 5 and 6 show the dependence of the magnetic force F and average magnetic flux density B_{avrg} in the permanent magnet on the releasing pulse current density J_{off} for both arrangements in Fig. 2.

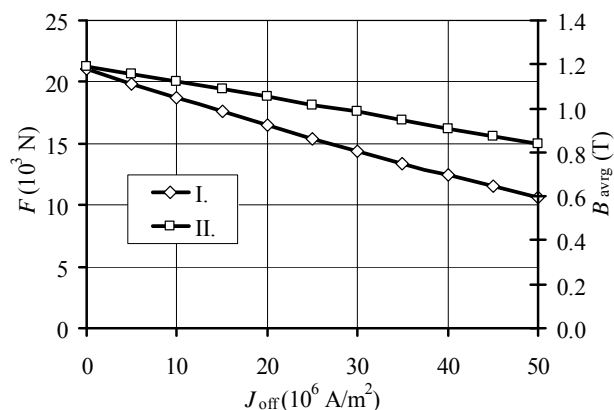


Fig. 5. Basic static demagnetization characteristic of the fixing element in the basic version (Fig. 2 on the left)

$b_1 / a_1 = 80 / 40$, $\delta = 2$ mm - see Fig. 1: I – F , II – B_{avrg}

In comparison with the original arrangement (Fig. 2 left), the improved arrangement (Fig. 2 right) is characterized by higher magnetic force F . This is due to the suppression of the leakage field in the thinner air gap. On the other hand, the average magnetic flux density B_{avrg} in the permanent magnet remains almost the same, which is favorable from the viewpoint of its deterioration due to demagnetization during the process of switching off the element.

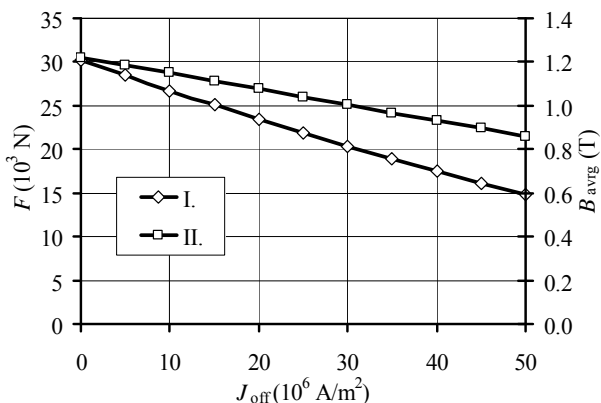


Fig. 6. Basic static demagnetization characteristic of the fixing element in the improved version (Fig. 2 on the right)
 $b_1 / a_1 = 80 / 40$, $\delta = 2$ mm - see Fig. 1: I - F , II - B_{avg}

The influence of the dimensions a_1 and b_1 of the permanent magnet can be seen in Figs. 7 and 8. Figure 7 shows that its width a_1 has a substantial influence only in the case that a_1 is smaller than the width of the rail. In the opposite case, magnetic field produced by the permanent magnet leaks into air surrounding the front of the rail and exhibits practically no influence on the force F . Analogously, Fig. 8 shows that the height b_1 of the permanent magnet has a visible influence only for smaller values of b_1 . For greater values of this parameter its influence on the force F (practically negligible).

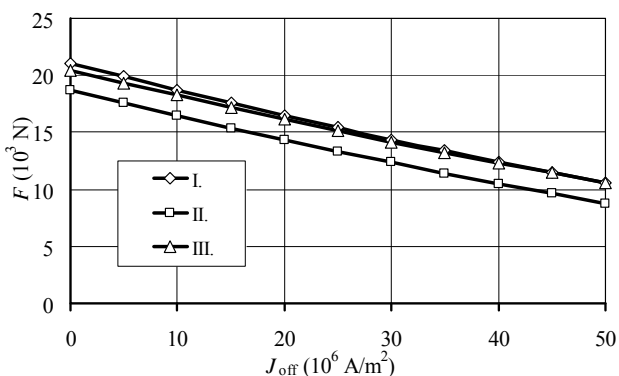


Fig. 7. Influence of the dimension a_1 (width) of the permanent magnet on its static demagnetization characteristic ($\delta = 2$ mm)
 I - $b_1 / a_1 = 80 / 40$ mm (starting relation), II - $b_1 / a_1 = 80 / 30$ mm,
 III - $b_1 / a_1 = 80 / 50$ mm

Another interesting quantity is the thickness δ of the nonmagnetic gap. Its influence on the magnetic force F is presented in Fig. 9. It is clear that growing thickness δ of the gap negatively affects this force, because the reluctance of the flux path increases. The exchangeable spacer **5.2**, therefore, should be as thin as possible. But from the viewpoint of protecting the permanent magnet from possible mechanical damaging due to undesirable contact with the polluted front of the rail the spacer must be made of a sufficiently thick metal sheet.

Conclusion

The investigated device for transporting long bodies (rods, rails) working with permanent magnets is not only very simple from the constructional viewpoint, but also it

exhibits very good operation properties. If the mass of one-meter rail is 70 kg, we need (in the improved arrangement) only two permanent magnets of total length, say, 60 mm, which secures the coefficient of security almost 3. Moreover, the device does not need any external source of current. Next work in the field will be focused on the design of the source of pulsed demagnetizing current I_{off} and also on experimental verification of the calculated results.

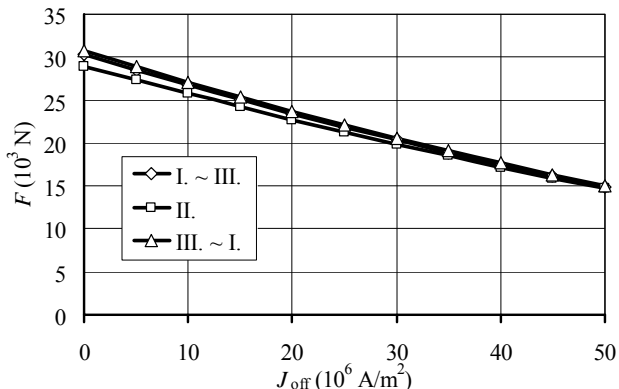


Fig. 8. Influence of the dimension b_1 (height) of the permanent magnet on its static demagnetization characteristic ($\delta = 2$ mm)
 I - $b_1 / a_1 = 80 / 40$ mm (starting relation), II - $b_1 / a_1 = 40 / 40$ mm,
 III - $b_1 / a_1 = 120 / 40$ mm

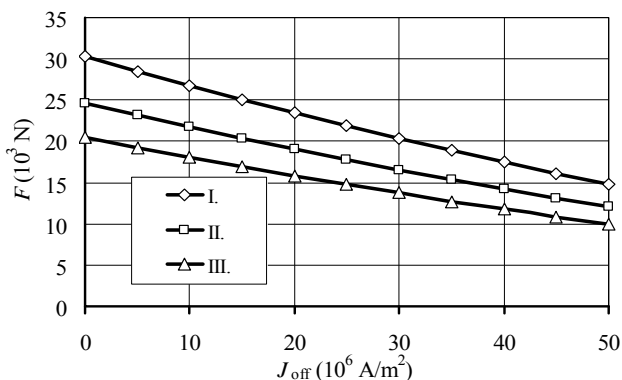


Fig. 9. Influence of the thickness δ of the nonmagnetic spacer **5.2** (Fig. 1) on the static demagnetization characteristic of the element in the improved arrangement, $b_1 / a_1 = 80 / 40$: I - $\delta = 2$ mm, II - $\delta = 3$ mm, III - $\delta = 4$ mm

Acknowledgment

This work was supported by the Grant project GAČR P102/11/0498.

REFERENCES

- [1] Kuczmann, M. Iványi, A.: *The Finite Element Method in Magnetics*, Akadémiai Kiadó, Budapest, 2008.
- [2] Furlani, E. P.: *Permanent Magnet and Electromechanical Device*. Academic Press, New York, 2001.
- [3] Materials of company Chen Yang Technologies, GmbH & Co. KG, <http://www.cy-magnetics.com>.
- [4] ŠKODA Company Standard ŠKODA 00 6004.
- [5] Code QuickField, <http://www.quickfield.com>.

Authors: Prof. Ing. Ivo Doležel, CSc., Czech Technical University, Faculty of Electrical Engineering, Technická 2, 166 27 Praha 6, Czech Republic, E-mail: dolezel@fel.cvut.cz, Dr. Martin Škopek, Assoc. Prof. Bohuš Ulrych, CSc., University of West Bohemia, Faculty of Electrical Engineering, Univerzitní 26, 306 14 Plzeň, Czech Republic, E-mail: [skopek, ulrych}@kte.zcu.cz](mailto:{skopek, ulrych}@kte.zcu.cz).